Supplementary Figure 1

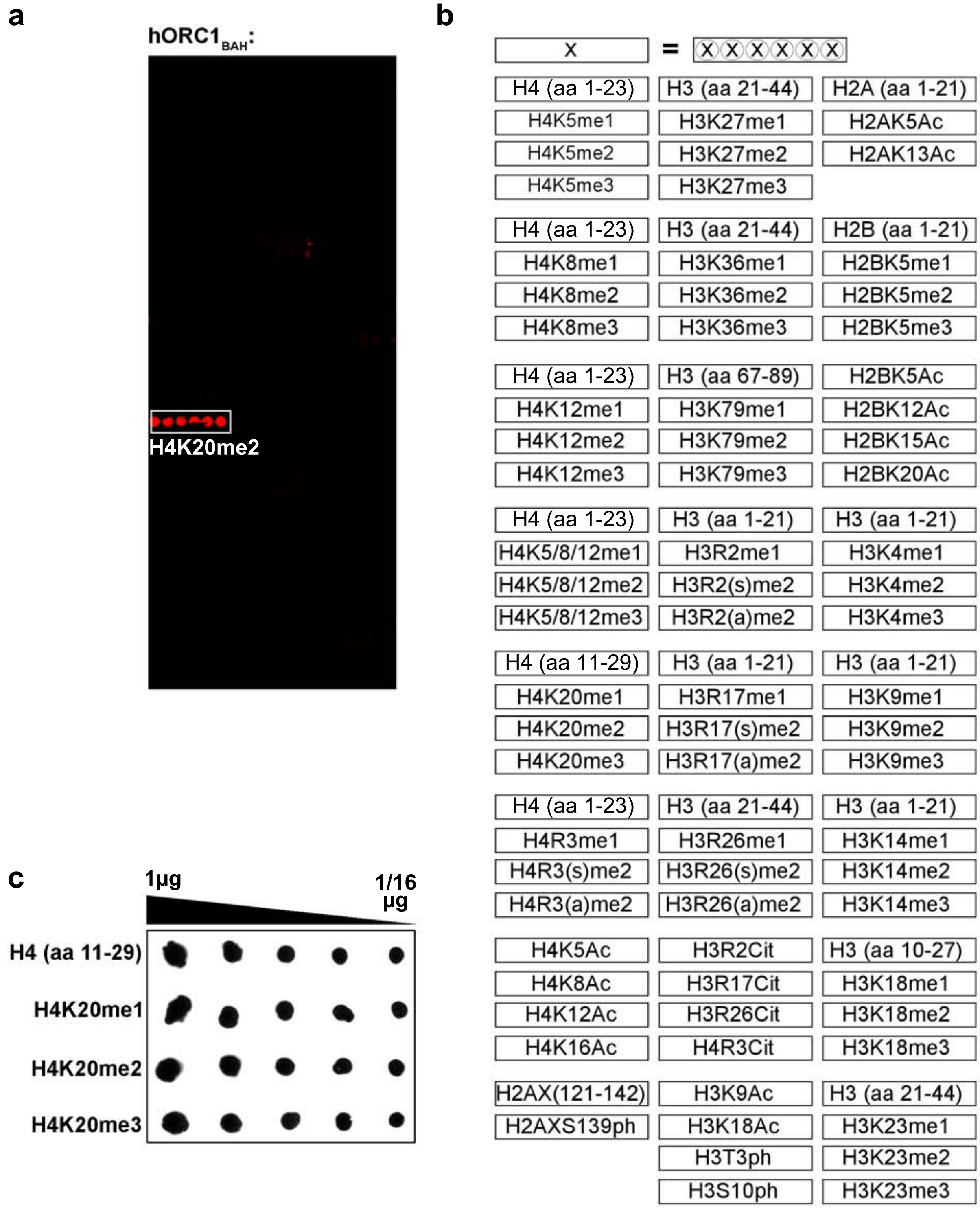

Supplementary Figure 1. hORC1$_{BAH}$ preferentially binds H4K20me2. a, Independent replica of data in Figure 1a, showing hORC1$_{BAH}$ preferential binding to H4K20me2 on peptide microarrays. **b**, Schematic of the histone peptides spotted on the histone peptide microarrays. **c**, The indicated biotinylated histone peptides used in peptide pull-down assays (Fig. 1c, 1f, 2g, and 4c) were spotted onto nitrocellulose membrane in serial dilution and detected with streptavidin-HRP.

Supplementary Figure 2

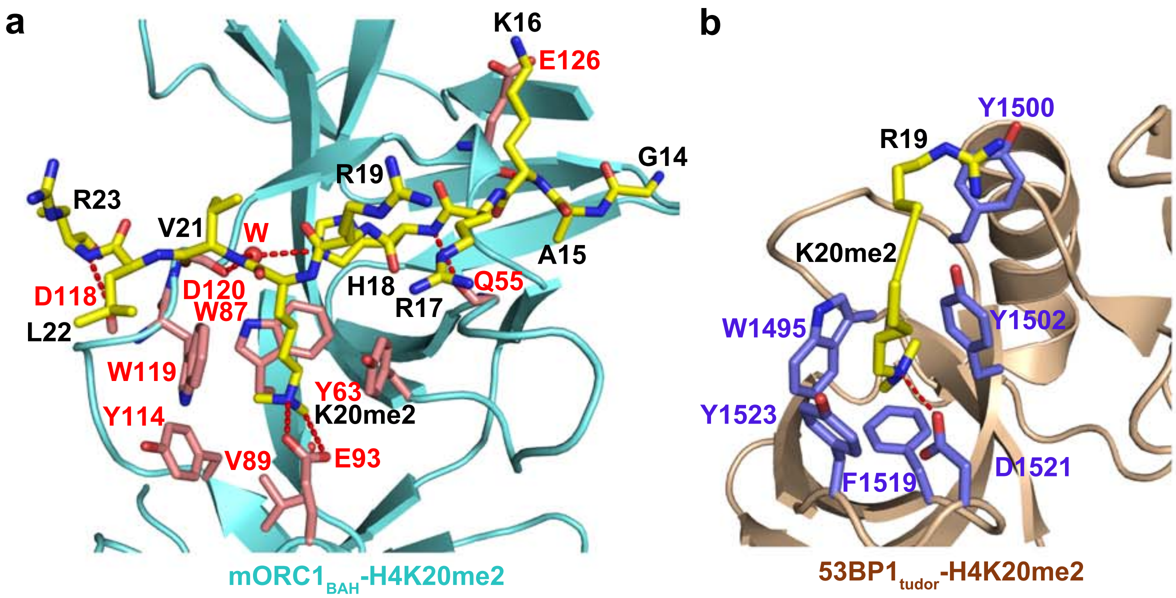

Supplementary Figure 2. Comparison of intermolecular contacts between mORC1$_{BAH}$-H4K20me2 and 53BP1 tudor domain (53BP1$_{tudor}$)-H4K20me2 complexes. a, Details of intermolecular contacts in the mORC1$_{BAH}$-H4K20me2 complex, the same as shown in Fig. 2b. **b**, Details of intermolecular contacts in the 53BP1$_{tudor}$-H4K20me2 complex (PDB 2IG0). 53BP1$_{tudor}$ and H4K20me2 peptide residues are colored in blue and yellow, respectively, with hydrogen bonds depicted as red dashed lines. Structural comparison of these two complexes indicates that both mORC1$_{BAH}$ and 53BP1$_{tudor}$ adopt an aromatic cage, adjoined by an acidic residue, to specifically recognize the H4K20me2 mark. However, the two proteins engage in distinct sequence specific interactions with the H4K20me2 peptide. In the mORC1$_{BAH}$-H4K20me2 complex, a fragment encompassing residues 16-23 of H4 is involved in intermolecular contacts with mORC1$_{BAH}$. By contrast, only residues H4R19 and H4K20me2 appear to interact with 53BP1$_{tudor}$ in the 53BP1$_{tudor}$-H4K20me2 complex. Notably, residue H4R19 associates with Tyr1500 of 53BP1$_{tudor}$ through a cation-π interaction in the latter complex, unlike that in the mORC1$_{BAH}$-H4K20me2 complex where its side chain is left exposed to the solvent.

Supplementary Figure 3

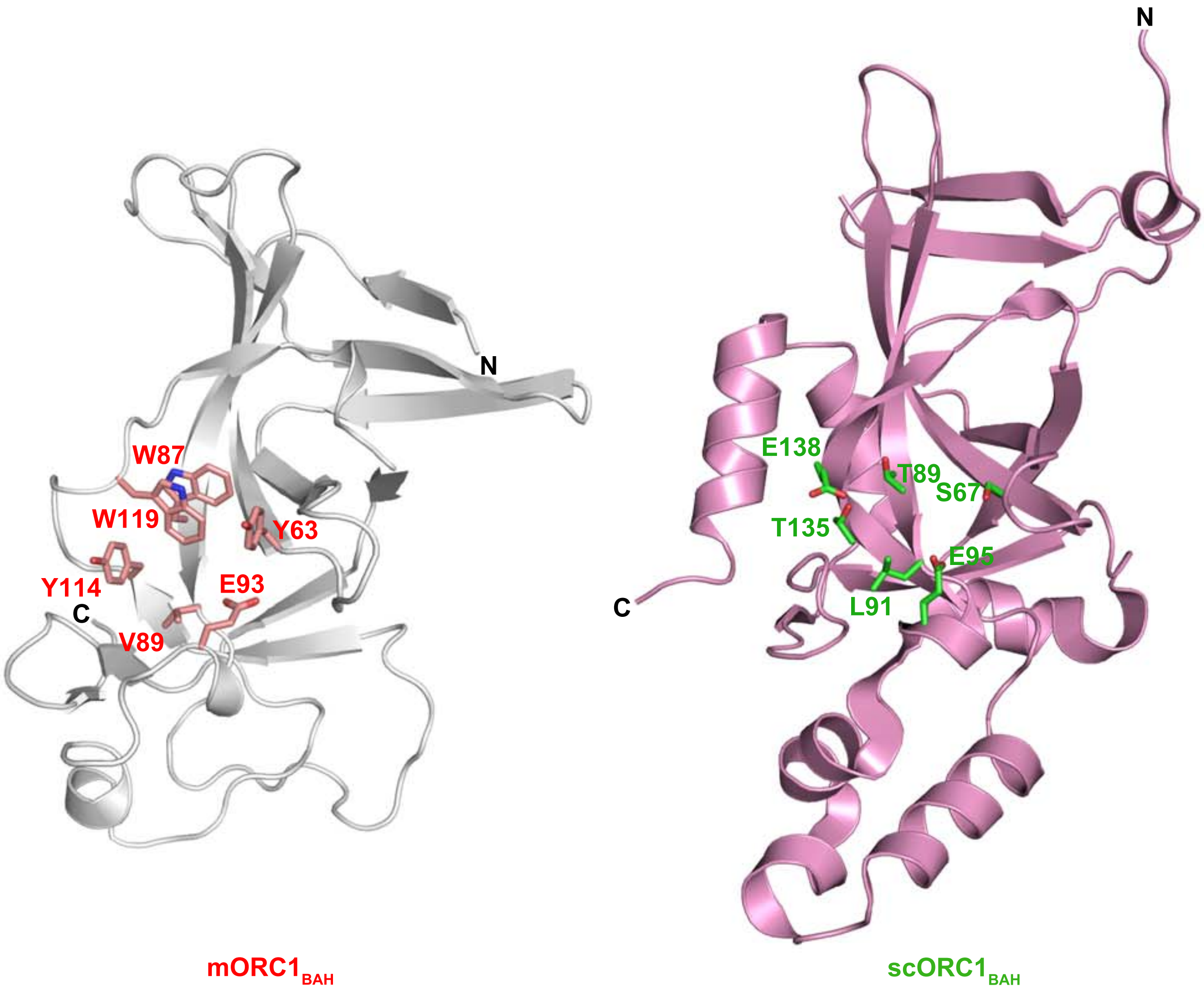

Supplementary Figure 3. **Structural comparison of mORC1$_{BAH}$ and scORC1$_{BAH}$.** The residues lining the H4K20me2-binding cage of mORC1$_{BAH}$ are colored in pink, and the residues in the corresponding positions in scORC1$_{BAH}$ are colored in green. Comparison of these two structures indicates that scORC1$_{BAH}$ does not form an aromatic cage to harbor H4K20me2, explaining why scORC1$_{BAH}$ is incapable of binding to H4K20me2.

Supplementary Figure 4

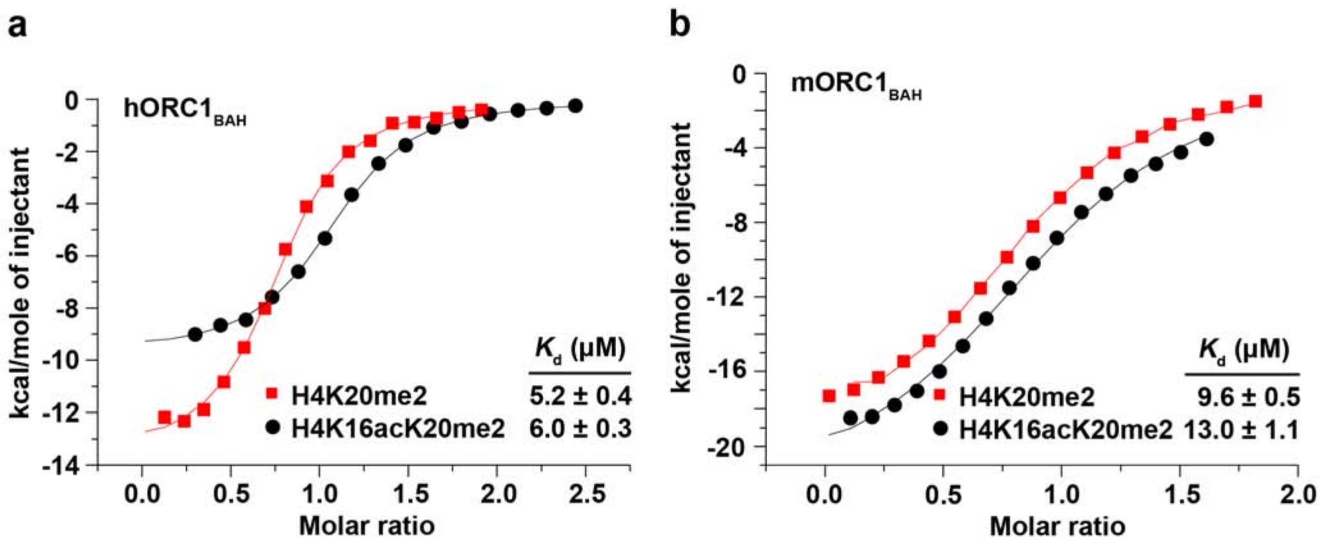

Supplementary Figure 4. **Impact of H4K16 acetylation on h(m)ORC1$_{BAH}$-H4K20me2 interaction**. **a**, ITC analysis of the interactions of hORC1$_{BAH}$ with H4K20me2 (red squares) and H4K20me2 acetylated at H4K16 (H4K16acK20me2, black circles) peptides. The ITC data for wild-type hORC1$_{BAH}$ is reproduced from Fig. 1d. **b**, ITC analysis of the interactions of mORC1$_{BAH}$ with H4K20me2 (red squares) and H4K16acK20me2 (black circles) peptides. These results indicate that acetylation of H4K16 resulted in slightly weaker binding (higher K_d values) for both hORC1$_{BAH}$-H4K20me2 and mORC1$_{BAH}$-H4K20me2 complexes.

Supplementary Figure 5

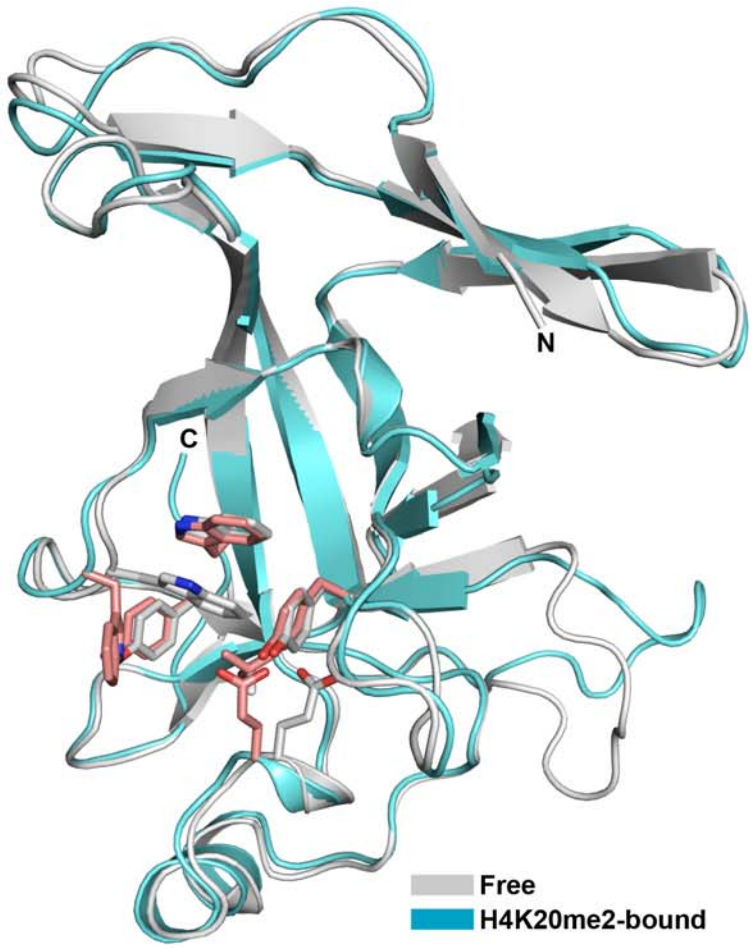

Supplementary Figure 5. The structural overly between free and H4(14-25)K20me2-bound $mORC1_{BAH}$ domains. The residues forming the H4K20me2-binding pocket are shown in stick representation, colored silver in free state and salmon in the H4K20me2-bound state.

Supplementary Figure 6

a

Peptide	K_d ± s.d. (μM)			
	Wild-type $mORC1_{BAH}$	W119C $mORC1_{BAH}$	Wild-type $hORC1_{BAH}$	C120A $hORC1_{BAH}$
H4K20me1	32.7 ± 1.4	40.5 ± 3.0	24.8 ± 3.8	308.0 ± 21.0
H4K20me2	9.6 ± 0.5	11.0 ± 1.2	5.2 ± 0.4	27.4 ± 4.4
H4K20me3	17.4 ± 0.9	32.3 ± 3.7	40.0 ± 7.0	319.0 ± 46.0

b

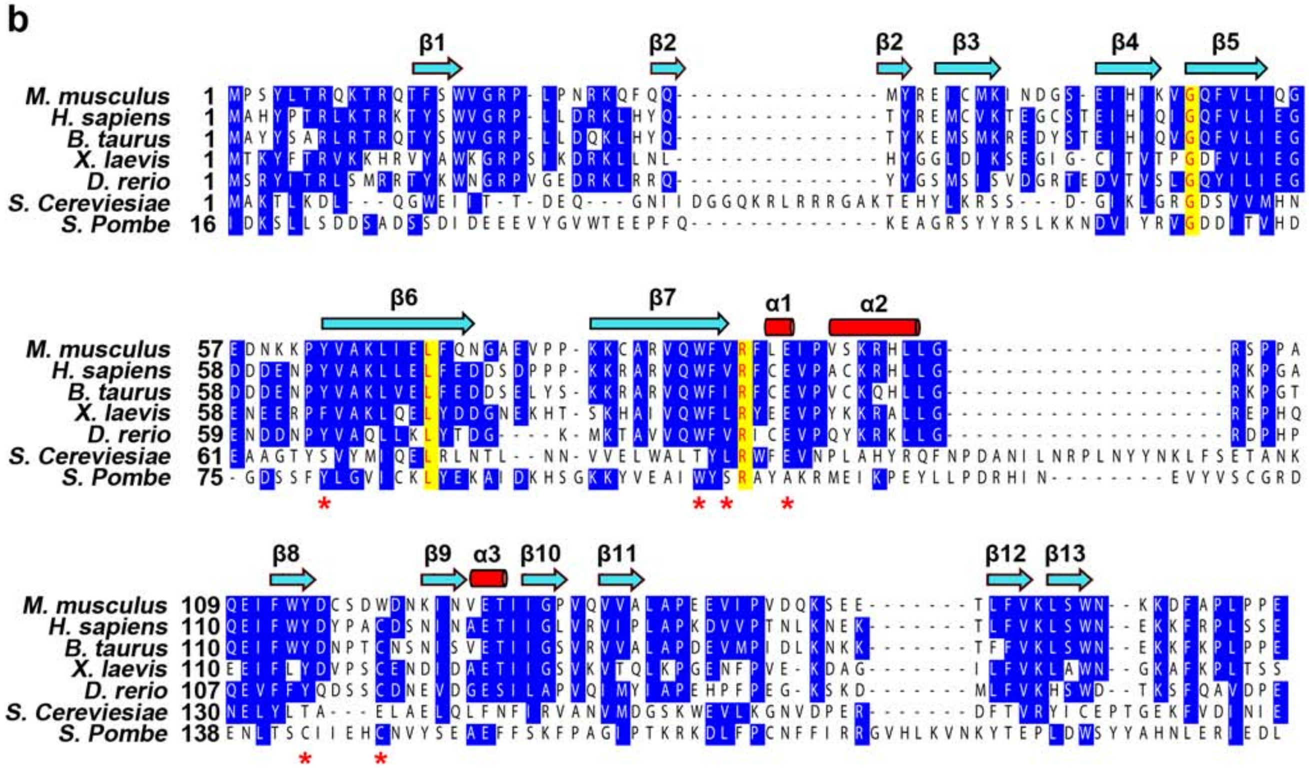

c

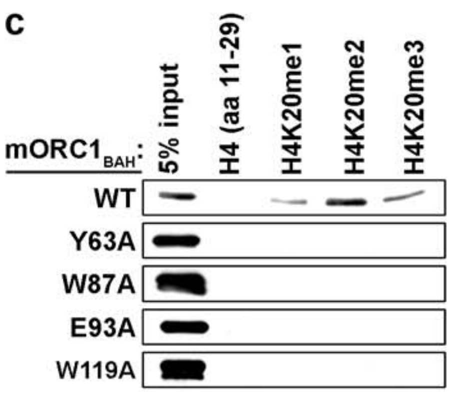

Supplementary Figure 6. **Evolutionary conservation of the ORC1 BAH domain**. **a**, Binding affinities of $mORC1_{BAH}$, $mORC1_{BAH}$ W119C mutant, $hORC1_{BAH}$ and $hORC1_{BAH}$ C120A mutant for the indicated H4K20 peptides determined by ITC as in (Fig. 1d). Note that replacement of Trp119 of $mORC1_{BAH}$ with a cysteine slightly improves its discrimination of H4K20me2 against H4K20me3. **b**, Sequence alignment of $ORC1_{BAH}$ for listed species using Clustal W. Completely conserved residues are colored in red and highlighted in yellow. Identical or similar residues are highlighted in blue. H4K20me2-binding residues are indicated with a red asterisk (*). Note that these residues are not well conserved in $scORC1_{BAH}$ and $spORC1_{BAH}$. α, alpha-helix. β, beta-sheet. **c**, Peptide-binding assays of $mORC1_{BAH}$ mutants with the indicated peptides.

Supplementary Figure 7

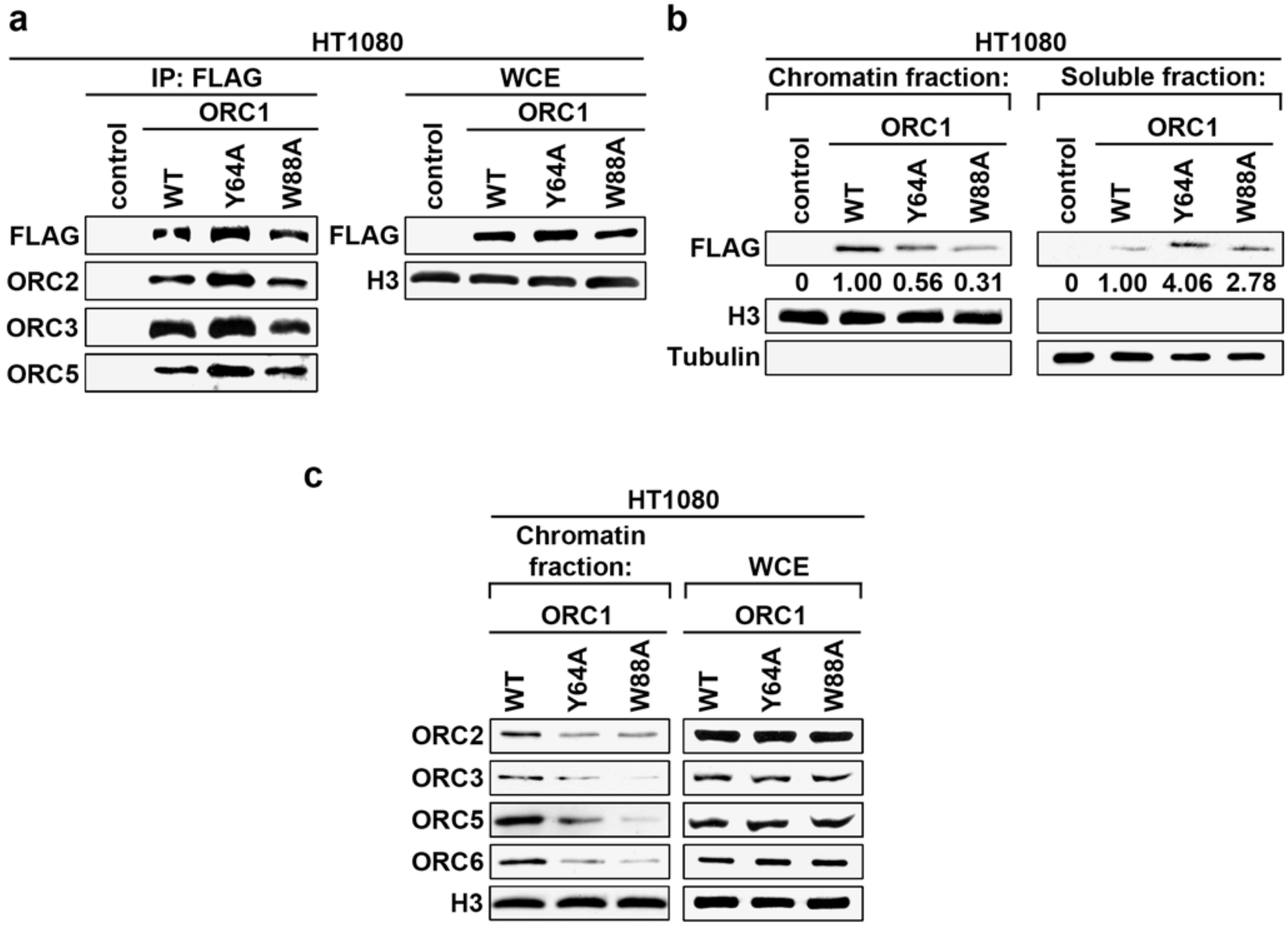

Supplementary Figure 7. ORC1-H4K20me2 interaction regulates ORC chromatin association. a, Western blot analysis with the indicated antibodies of wild-type (WT) and H4K20me2-binding pocket mutants (Y64A and W88A) affinity-purified FLAG-tagged ORC1 complexes from HT1080 cells. Control, empty vector control IP. WCE, whole cell extract. **b,** The $ORC1_{BAH}$-H4K20me2 interaction is required for efficient ORC1 chromatin association. Western blot analysis of lysates biochemically separated into chromatin-enriched and soluble fractions from HT1080 cells stably expressing the indicated ORC1 protein. Quantitation of FLAG-ORC1 levels is shown. Control, empty vector control lysates. Tubulin and H3 levels are shown as control for the integrity of fractionation. **c,** Disruption of ORC1 binding to H4K20me2 destabilizes ORC chromatin association. Western blot analysis of biochemically purified chromatin from HT1080 cells as in (b) with the indicated antibodies. Total ORC protein levels in WCE are shown.

Supplementary Figure 8

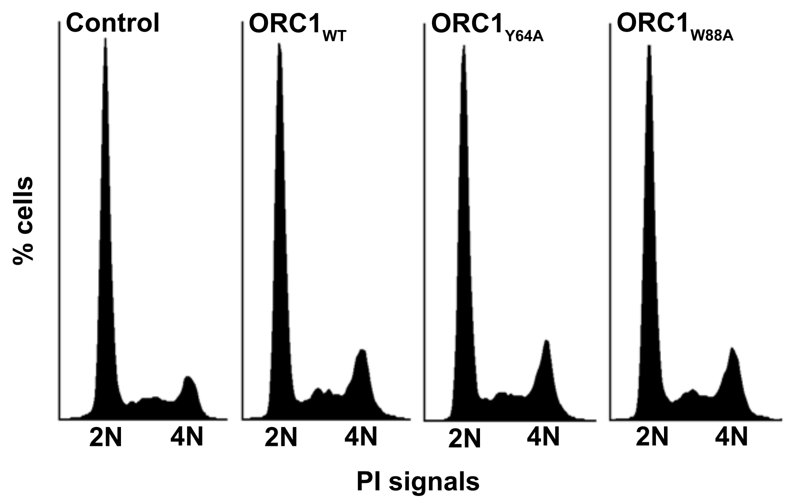

Supplementary Figure 8. Flow cytometry analysis of U2OS cells synchronized in G1 phase of the cell cycle. U2OS cells stably expressed the indicated ORC1 protein used for the experiments in Figure 3d and 3e were synchronized in M-phase with nocodazole and released into G1-phase (see Methods). The cell-cycle profiles were determined by PI staining followed by flow cytometry.

Supplementary Figure 9

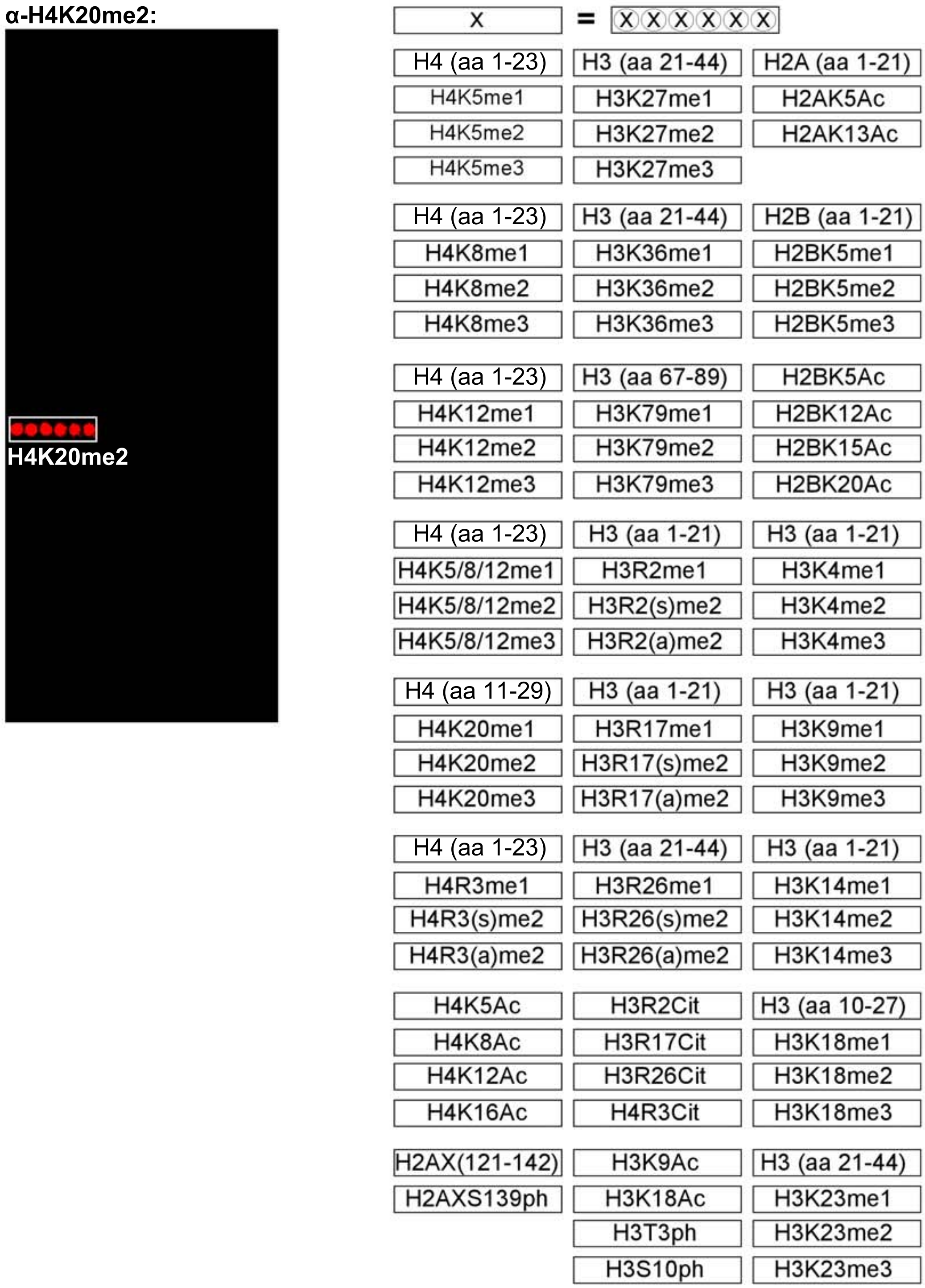

Supplementary Figure 9. H4K20me2 antibody shows specific binding to H4K20me2 peptide. Peptide microarray analysis of H4K20me2 rabbit polyclonal antibody used for ChIP assays in Fig. 3d-e (left). Schematic of the histone peptides spotted on the histone peptide microarrays (right).

Supplementary Figure 10

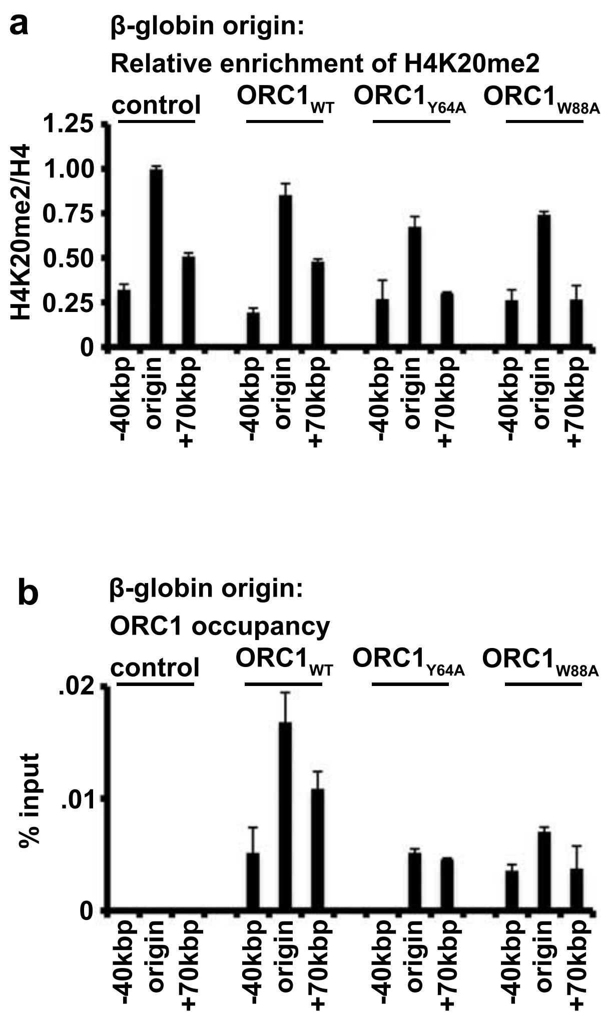

Supplementary Figure 10. H4K20me2 is enriched at DNA replication origins and an intact BAH domain is required for ORC1 occupancy at replication origins. a, ChIP analyses of H4K20me2 signals at the β-globin origins and the indicated flanking regions in G1 phase synchronized U2OS cells stably expressing the indicated ORC1 protein; *y*-axis: H4K20me2 ChIP/H4 ChIP. **b,** Occupancy of FLAG tagged hORC1, $hORC1_{Y64A}$, $hORC1_{W88A}$, or control was determined by ChIP analysis (*y*-axs: % input) at the indicated origins as in (a). Error bars in (a, and b,) indicate s.e.m. from three experiments.

Supplementary Figure 11

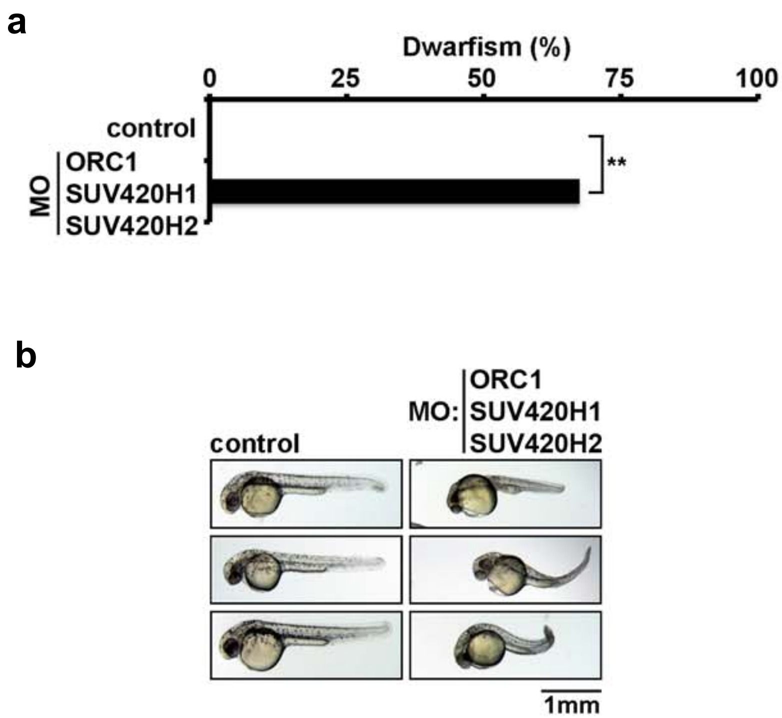

Supplementary Figure 11. ***orc1/suv4-20h1/h2* morphants do not display significantly more dwarfism than *orc1* or *suv4-20h1/h2* morphants. a**, Quantification of dwarf phenotype in zebrafish injected with morpholino oligos (MO) targeting the *Orc1*, *Suv4-20h1* and *Suv4-20h2* translation start sites as in Figure 4. Control, uninjected embryos. Zebrafish analyzed: control: 54; MO: 126. ** $P < 0.01$. **b**, representative images of zebrafish in (a) 1 day post-fertilization.

Supplementary Table 1

	$mORC1_{BAH}$	H4(14-25)K20me2-$mORC1_{BAH}$
Data collection	**SeMet**	**Native**
Wavelength (Å)	0.9792	0.9792
Space group	*P21*	*P1*
Cell dimensions		
a, *b*, *c* (Å)	49.9, 53.9, 72.0	35.1, 49.4, 54.4
a, *b*, *g* (°)	90, 102.4, 90	89.9, 102.1, 103.3
Resolution (Å)*	30-1.7 (1.76-1.70)	30-1.95 (2.02-1.95)
R_{sym} or R_{merge}*	6.4 (44.5)	6.8 (25.3)
I/s*I*	24.3 (2.8)	12.3 (2.8)
Completeness (%)*	99.5 (100.0)	96.9 (95.8)
Redundancy*	3.7 (3.7)	2.1 (2.0)
Unique reflections	41,079 (4,090)	25,244 (2,482)
Refinement		
Resolution (Å)	22.4-1.7	25.9-1.95
No. reflections	41,016	24,544
$R_{work/}$ R_{free}	21.5/24.3	21.3/25.7
No. atoms		
Protein	2,467	2,490
Water	240	196
Peptide		386
B-factors		
Protein	30.3	40.9
Water	38.9	43.9
Peptide		47.2
R.m.s deviations		
Bond lengths (Å)	0.007	0.011
Bond angles (º)	1.120	1.408

*Highest resolution shell is shown in parenthesis.